Journal of Solid State Chemistry 181 (2008) 3322–3326

Contents lists available at ScienceDirect

Journal of Solid State Chemistry

journal homepage: www.elsevier.com/locate/jssc

A two-fold interpenetrating 3D metal-organic framework material constructed from helical chains linked via 4,4′-H_2bpz fragments

Yi-Ming Xie [a,b], Zhen-Guo Zhao [a], Xiao-Yuan Wu [a], Qi-Sheng Zhang [a], Li-Juan Chen [a], Fei Wang [a], Shan-Ci Chen [a], Can-Zhong Lu [a,*]

[a] State Key Laboratory of Structural Chemistry, Fujian Institute of Research on the Structure of Matter, Chinese Academy of Sciences, Fuzhou, Fujian 35002, China
[b] College of Materials Science and Engineering, Huaqiao University, the Key Laboratory for Functional Materials of Fujian Higher Education, Quanzhou, Fujian 362021, China

ARTICLE INFO

Article history:
Received 13 June 2008
Received in revised form
3 September 2008
Accepted 7 September 2008
Available online 30 September 2008

Keywords:
Crystal structure
Helical chains
Metal-organic
Photoluminescence

ABSTRACT

A 3-connected dia-f-type metal-organic framework compound $\{[Ag(L)_{3/2}H_2PO_4]\}_n$ (**1**) has been synthesized by self-assembly of 4,4′-H_2bpz (L = 4,4′-H_2bpz = 3,3′,5,5′-tetramethyl-4,4′-bipyrazole) and $Ag_4P_2O_7$ under hydrothermal conditions. It crystallizes in the tetragonal space group $I4_1/acd$ with $a = 21.406(4)$ Å, $b = 21.406(4)$ Å, $c = 36.298(8)$ Å, $Z = 32$. X-ray single-crystal diffraction reveals that **1** has a three-dimensional framework with an unprecedented alternate left- and right-handed helices structure, featuring a non-uniform two-fold interpenetrated (4.14^2) net. Photoluminescent investigation reveals that the title compound displays interesting emissions in a wide region, which shows that the title compound may be a good potential candidate as a photoelectric material.

© 2008 Elsevier Inc. All rights reserved.

1. Introduction

The syntheses and characterizations of new crystalline porous materials, either with inorganic or metal-organic frameworks (MOFs), are of currently significant interest, of which the main focus is at new functional materials ranging from zeolite-analogues [1–6] to biomaterials [7–9], not only because of their intriguing architectures, but also of their tremendous potential applications in many fields [10–13]. However, in comparison with the above materials with inorganic frameworks, there have been much fewer examples of three-dimensional (3D) covalent MOFs, homochiral inorganic-organic hybrids in particular [14]. An attractive and structurally simple bifunctional tecton for the generation of helical architectures is 3,3′,5,5′-tetramethyl-4,4′-bipyrazole (4,4′-H_2bpz) [15]. By the combination of the inherent functional features of the organic and inorganic counterparts, it has generated the target coordination network with a new dia-f topology. The desired connectivity may be tuned by the conformational flexibility of the organic linker. First of all, the 4,4′-bpz acts as an angular linker. Its frame includes two planar pyrazolyl fragments, which have an angle of rotation around 50–90° [16] and result non-collinear orientation of two N–M vectors, making it possible for the assembly of the desired helical chains [17]. Furthermore, these coordination infinite right-handed or left-handed helical chains $[M(4,4'\text{-bpz})]_n$ that are formed by the tetrahedronally coordinated silver ions and one bridging 4,4′-bpz ligands, have a rich and versatile functionality for cross-linking into 3D MOFs. It is reported herein a MOF with an unusual two-fold interpenetrating dia-f topology, $\{[Ag(4,4'\text{-}H_2bpz)_{3/2}H_2PO_4]\}_n$ (**1**) [4,4′-H_2bpz = 3,3′,5,5′-tetramethyl-substituted 4,4′-bipyrazole], which is constructed by alternating left- and right-handed helical chains $\{[Ag(4,4'\text{-}H_2bpz)H_2PO_4]_n\}$ and the bridge ligand 4,4′-H_2bpz.

2. Experimental

2.1. Materials and methods

The attractive ligand 4,4′-H_2bpz was prepared according to the literature [18] and satisfactorily characterized by elemental analysis and IR. Other reactants of A.R. grade were obtained commercially and used without further purification. Elemental analyses were performed on a Vario EL III elemental analyzer. Infrared spectra were obtained with a PE Spectrum-One FT-IR spectrometer using KBr discs. The fluorescent data were collected at room temperature on a computer-controlled JY FluoroMax-3 spectrometer. Thermal stability studies were carried out on a NETSCHZ STA-449C thermoanalyzer under an N_2 atmosphere (30–1000 °C) at a heating rate of 10 °C min^{-1}. The UV–vis spectra were recorded at room temperature on a computer-controlled PE Lambda 900 UV–vis spectrometer equipped with an integrating

* Corresponding author. Fax: +86 591 83705794.
E-mail addresses: czlu@fjirsm.ac.cn, czlu@ma.fjirsm.ac.cn (C.-Z. Lu).

0022-4596/$ - see front matter © 2008 Elsevier Inc. All rights reserved.
doi:10.1016/j.jssc.2008.09.008

sphere in the wavelength range 190–1100 nm. $BaSO_4$ plate was used as a reference (100% reflectance), on which the finely ground powder of the samples were coated. The absorption spectra were calculated from reflection spectra by the Kubelka–Munk function [19]: $\alpha/S = (1-R)^2/2R$, where α is the absorption coefficient, S is the scattering coefficient which is practically wavelength independent when the particle size is larger than 5 μm, and R is the reflectance.

2.2. Synthesis of $\{[Ag(4,4'\text{-bpz})_{3/2}H_2PO_4]\}_n$ (**1**)

The title compound was prepared by mixing $Ag_4P_2O_7$ (0.605 g, 1 mmol) and 4,4′-H_2bpz (0.095 g, 0.5 mmol) in ethanol (5 mL) and H_2O (5 mL), heated in a 23 mL capacity Teflon-lined reaction vessel at 170 °C for 5 days. Then the autoclave was cooled at 5 °C h^{-1} to room temperature. The colorless block crystals of the title compound were isolated, washed with water and ethanol, and dried at room temperature. Yield: 0.22 g (34.7% based on Ag). Anal. Calcd. (%) for $C_{15}H_{23}AgN_6O_4P$: H: 4.74, C: 36.81, N: 17.18, P: 6.33, Ag: 21.86. Found: H: 4.86, C: 36.88, N: 17.20, P: 6.35, Ag: 21.85. IR spectrum (KBr pellets, ν/cm^{-1}): 3082(s, ν(= N–H)), 2974(s, $\nu(CH_3)$), 2926(br, $\nu(CH_3)$), 1650(s, ν(C═C)), 1417(s, $\nu(CH_3)$), 1384(s, $\nu(CH_3)$), 1302(s, ν(P═O)), 1160(w), 1089(w), 1050(s, ν(P–O)), 1017(w), 941(w), 880(s, ν(C═C)), and 778(w).

2.3. Crystal structure determination

X-ray diffraction data were collected on Rigaku Mercury CCD X-ray diffractometer with graphite monochromated Mo-$K\alpha$ radiation ($\lambda = 0.71073$ Å) using a ω scan technique. CrystalClear software was used for data reduction and empirical absorption correction. The structure was solved by the direct methods using the Siemens SHELXTL™ Version 5 package of crystallographic software [20]. The difference Fourier maps based on the atomic positions yield all non-hydrogen atoms. The hydrogen atom positions were generated theoretically, allowed to ride on their respective parent atoms and included in the structure factor calculations with assigned isotropic thermal parameters but were not refined. The structure was refined using a full-matrix least-squares refinement on F^2. All non-hydrogen atoms were refined anisotropically. The summary of crystallographic data and structure analysis is given in Table 1. The selected bond lengths and bond angles are listed in Table 2.

Table 1
Crystal data and structure refinement details for **1**

Formula	$C_{15}H_{23}AgN_6O_4P$
Mr	490.23
Color	Colorless
Crystal size (mm^3)	0.4, 0.38, 0.35
Crystal system	Tetragonal
Space group	$I4_1/acd$
a (Å)	21.406(4)
b (Å)	21.406(4)
c (Å)	36.298(8)
V ($Å^3$)	16633(6)
Z	32
$2\theta_{max}$ (°)	55
Reflections collected	59433
Independent, observed reflections (R_{int})	4770, 4517 (0.0228)
$d_{calcd.}$ (g cm^{-3})	1.566
μ (mm^{-1})	1.078
T (K)	293(2)
F(000)	7968
$R_1[I>2\sigma(I)]$, wR_2(all data)	0.0366, 0.0974
S	1.051
Largest and mean Δ/σ	0.003, 0.000
$\Delta\rho$(max/min) (e $Å^{-3}$)	1.063/−0.816

Table 2
Selected bond lengths (Å) and bond angles (°) for **1**

Ag(1)–N(5)	2.229(2)	Ag(1)–O(1)	2.520(2)
Ag(1)–N(1)	2.269(3)	Ag(1)–N(3)#1	2.382(2)
N(5)–Ag(1)–N(1)	124.90(9)	N(3)#1–Ag(1)–O(1)	96.30(8)
N(5)–Ag(1)–N(3)#1	103.0(1)	N(5)–Ag(1)–Ag(1)#2	86.10(6)
N(1)–Ag(1)–N(3)#1	94.1(1)	N(1)–Ag(1)–Ag(1)#2	78.34(6)
N(5)–Ag(1)–O(1)	119.15(8)	N(3)#1–Ag(1)–Ag(1)#2	170.54(8)
N(1)–Ag(1)–O(1)	110.21(9)	O(1)–Ag(1)–Ag(1)#2	81.27(4)

Symmetry codes: #1 $-y+3/4$, $x-1/4$, $-z+1/4$; #2 $-x+1$, $-y$, $-z$.

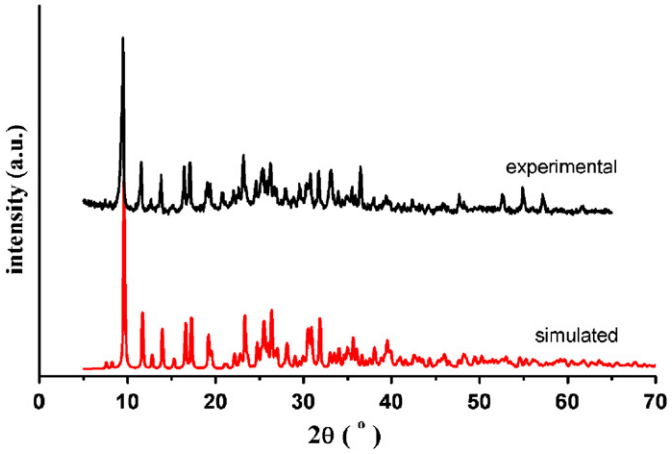

Fig. 1. Experimental and simulated X-ray powder diffraction patterns of compound **1**.

Powder X-ray diffraction (PXRD) patterns were measured on a Rigaku DMAX2500 powder diffractometer at 40 kV and 100 mA using Cu-$K\alpha$ ($\lambda = 1.54056$ Å), with a scan speed of 0.375 s/step and a step size of 0.05°. The simulated powder patterns were calculated using single-crystal X-ray diffraction data and processed by the free Mercury v1.4 program provided by the Cambridge Crystallographic Data Centre, as shown in Fig. 1.

Crystallographic data (excluding structure factors) for the structure reported in this paper is given in the appendix.

3. Results and discussion

The synthesis conditions for the title compound described in the Experimental section had been optimized for yields of crystalline products. This compound is very stable in air at ambient temperature and is almost insoluble in common solvents such as water, alcohol, acetonitrile, chloroform, acetone, toluene, etc.

Table 1 presents relevant crystallographic and refinement data. X-ray diffraction analysis reveals that the structure of the title compound is a two-fold interpenetrating 3D framework. Each silver atom is four-coordinated by one oxygen atom from H_2PO_4 and three nitrogen atoms from three 4,4′-H_2bpz ligands (Ag–N, 2.229(2)–2.382(2) Å; Ag–O, 2.5199(19) Å; N–Ag–N, 94.07(10)–124.90(9)°; N–Ag–O, 96.30(8)–119.15(8)°) in a distorted tetrahedral geometry (Fig. 2). The distance between Ag1⋯Ag1B is 3.2307(7) Å, which is markedly shorter than the sum of the van der Waals radii of two silver atoms (3.44 Å) [21], indicating a significant intramolecular Ag⋯Ag interaction. The 4,4′-H_2bpz ligand acts as a bridging linker that connects two Ag atoms, giving to the 3D framework depicted in Fig. 3. Notably, the dihedral angle between the plane formed by N1–N2–C2–C3–C4 (plane 1) of 4,4′-H_2bpz and the plane defined by N3–N4–C7–C8–C9 (plane 2) of

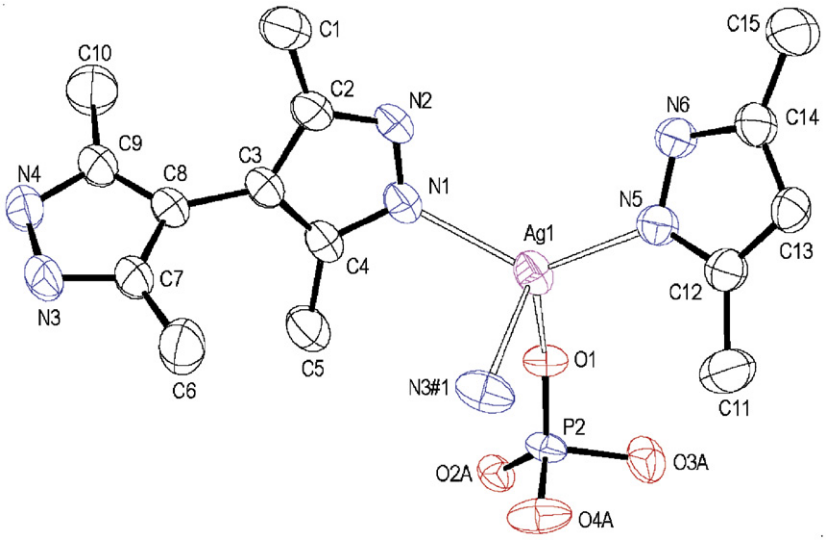

Fig. 2. ORTEP drawing of **1** with 50% thermal ellipsoids. Hydrogen atoms and disordered O2B, O3B, and O4B atoms are omitted for clarity (symmetry code: #1 3/4−*y*, −1/4+*x*, 1/4−*z*).

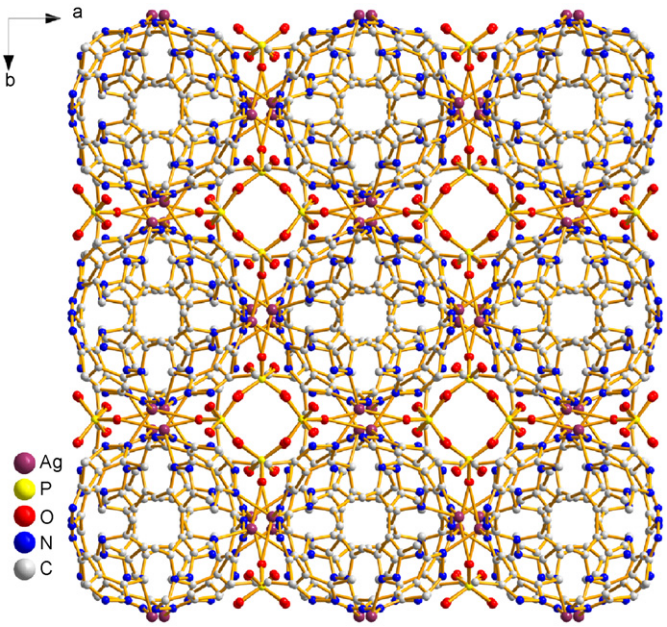

Fig. 3. 3D organic–inorganic porous framework of **1**.

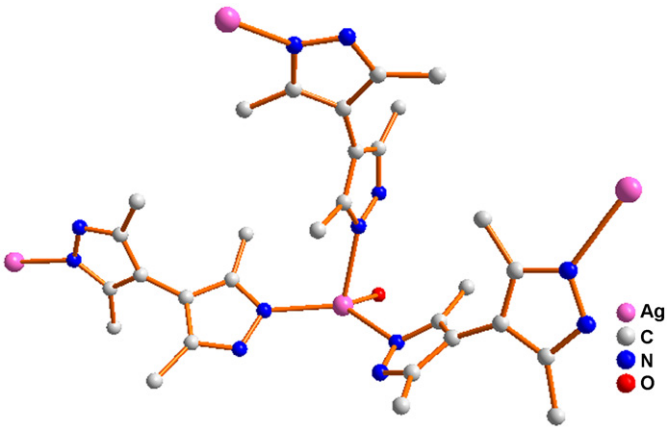

Fig. 4. The similar *cis*- and *trans*-models for the 4,4′-H_2bpz ligands in **1**.

4,4′-H_2bpz is 66.12°, while that between the planes 3 (defined by N5–N6–C12–C13–C14) and 4 (formed by N5E–N6E–C12E–C13E–C14E) is 67.35°. Unusually, the 4,4′-H_2bpz ligands connect the two silvers in a similar *cis* and *trans* arrangement (Fig. 4), which is quite different from those in the similar reported chains where only similar *cis* or *trans* arrangements were presented [16,22]. This results two lengths of Ag···Ag linked by 4,4′-H_2bpz bridge ligand, which are 10.0782 Å for *trans*-model and 9.4055 Å for *cis*-model.

The Ag atoms are alternately bridged by two or three μ_2-4,4′-H_2bpz ligands in a similar *trans*-mode or *cis*-mode to construct the infinite meso-helical chains along the *a* axial direction. Interestingly, such chains crystallize in both right- and left-handed fashions (Fig. 5). However, the right-handed helical chains are further linked only to the other four neighboring right-handed helical chains by the 4,4′-H_2bpz bridge ligands, not to the left-handed helical chains, and extended to a 3D network, so do the left-handed chains. It is notable that **1** exhibits a two-fold interpenetrating framework. To the best of our knowledge, only a few meso-helices have been reported and examples are usually 1D and 2D layers [23]. The title compound is a new 3D polymer built upon meso-helices up to now.

In order to illustrate this structure more simply, the 4,4′-H_2bpz bridge ligands are omitted due to their linear coordination geometry, the Ag atoms can be viewed as linked three-coordinate non-planar nodes with triangular-pyramidal geometry. A single 3D framework could be extended to a rare 4.14^2 net, as displayed in Figs. 5 and 6. The extended Schläfli symbol of this net is $4.14_{12}.14_{12}$, which is assigned to the dia-f net [24]. An interesting feature of this 4.14^2 net is the presence of the separated hexagonal single helices running along *a*-axis, which is highlighted in Fig. 6. Each hexagonal helix connects to four adjacent helices by sharing a common edge. These 4.14^2 nets are two-fold parallel interpenetrating along *a*-axis and interlocked to each other. The present net is strongly distorted and differs from the regular dia-f net, whose symmetrical configuration is normally $I4_1/amd$ of the tetragonal cell [25]. As far as now, only a few compounds of the 4.14^2 net have been reported [26].

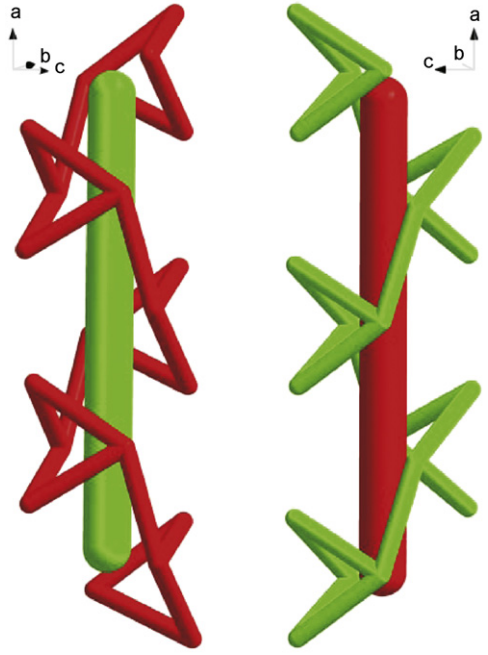

Fig. 5. Views of the left- (left) and right-hand (right) helices.

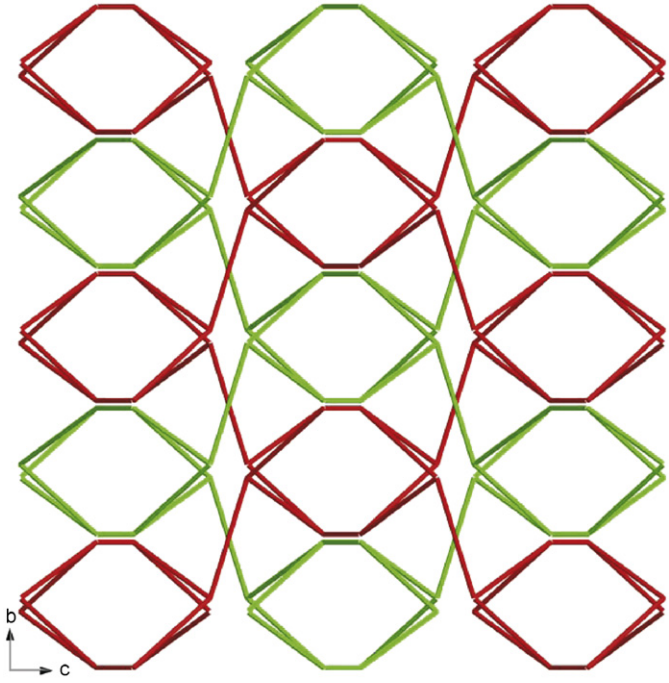

Fig. 6. Schematic view of the two-fold interpenetrated network.

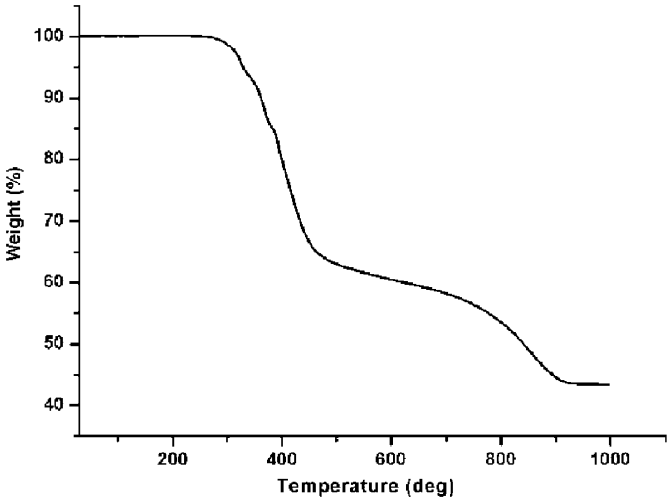

Fig. 7. TGA diagram of **1**.

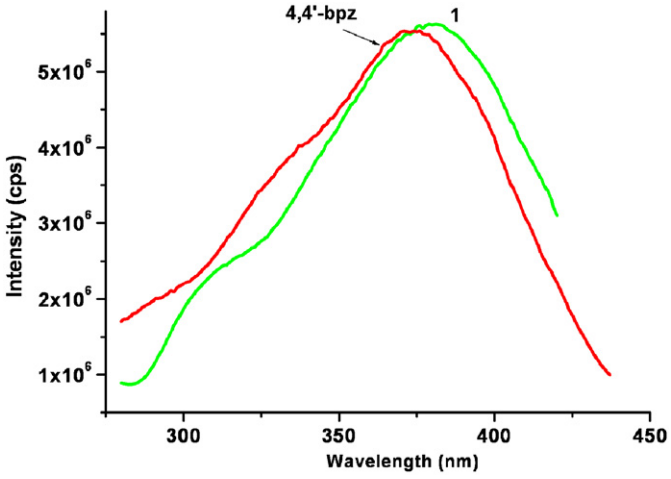

Fig. 8. Solid-state emission spectra of **1** and 4,4′-H_2bpz at room temperature.

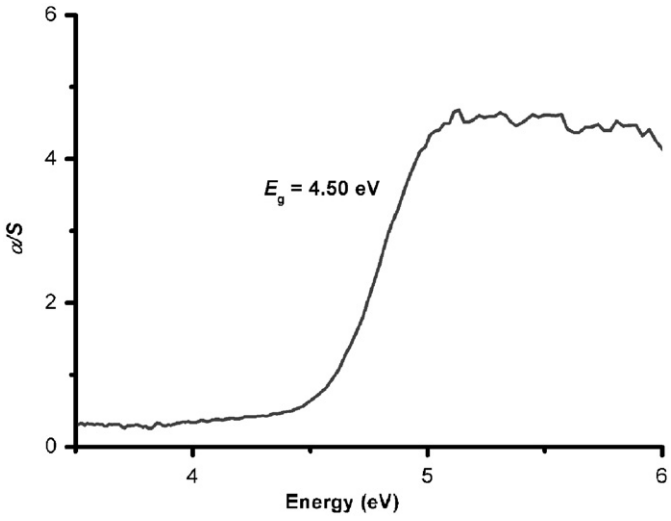

Fig. 9. Solid-state diffuse reflectance spectrum of **1**.

The thermal stability of compound **1** has been studied through TGA, which performed from 30 to 1000 °C. The TGA of compound **1** (Fig. 7) under a N_2 atmosphere demonstrates that the material is stable up to ca. 270 °C, whereupon the ligands lose in two stages: the first step is from 270 to 600 °C (39% weight loss observed, 38% theoretical), the second step is from 600 to 930 °C (17% weight loss observed, 18% theoretical), which might be owing to that the silver atoms linked by 4,4′-H_2bpz ligands have two coordination environments (the one distance of Ag⋯Ag is in 9.407 Å for the similar *cis*-mode and the other one is in 10.708 Å for the similar *trans*-mode, and it is well known that the *trans*-mode is more stable than the *cis* one). At last from 930 to 1000 °C, it keeps a constant and provides an amorphous powder finally.

Luminescent properties: Upon excitation at 360 nm, compound **1** displays an extensive blue luminescence emission in solid state at room temperature with a maximum at ca. 443 nm (Fig. 8). Since similar emissions with $\lambda_{max} = 457$ nm were also observed for 4,4′-H_2bpz in solid state. The fluorescent emission of **1** may be tentatively assigned to the intraligand transition of the free ligand fluorescent emissions [27]. Optical absorption spectrum of **1** reveals the presence of an obviously optical gap of 4.50 eV (Fig. 9), which suggests that compound **1** may be a potential wide-gap semiconductor and is consistent with the color of the crystal. The optical absorption of **1** is likely originated from ligand-centered π–π^* (LC) transitions.

4. Conclusions

In brief, we have successfully assembled a new MOF by exploitation of silver atoms as metal nodes and 4,4′-H_2bpz ligands as linkers under hydrothermal conditions. The title compound features a new two-fold interpenetrating 3D network structure with dia-f topological nets, constructed from unprecedented alternate right- or left-handed helical chains linked via 4,4′-H_2bpz fragments. The title compound may be a potential candidate as photoactive material owing to its fluorescence, thermal stability and insolubility in common polar and non-polar solvents.

Appendix A

Supplementary material CCDC 676218 contains the supplementary crystallographic data for **1**. These data can be obtained free of charge via http://www.ccdc.cam.ac.uk/conts/retrieving.html, or from the Cambridge Crystallographic Data Centre, 12 Union Road, Cambridge CB2 1EZ, UK; fax: (+44)1223-336-033; or e-mail: deposit@ccdc.cam.ac.uk.

Acknowledgments

This work was supported by the 973 key program of the MOST (2006CB932904, 2007CB815304), the National Natural Science Foundation of China (20425313, 20521101 and 50772113), Chinese Academy of Sciences (KJCX2-YW-M05) and the Natural Science Foundation of Fujian Province (2006L2005).

References

[1] S. Ma, D. Sun, X.S. Wang, H.C. Zhou, Angew. Chem. Int. Ed. 46 (2007) 2458.
[2] P. Feng, X. Bu, G.D. Stucky, Nature 388 (1997) 735.
[3] M. Eddaoudi, D.B. Moler, H.L. Li, B.L. Chen, T.M. Reineke, M. O'Keffe, O.M. Yaghi, Acc. Chem. Res. 34 (2001) 319.
[4] S.L. James, Chem. Soc. Rev. 32 (2003) 276.
[5] X.C. Huang, Y.Y. Lin, J.P. Zhang, X.M. Chen, Angew. Chem. Int. Ed. 45 (2006) 1557.
[6] D. Bradshaw, J.B. Claridge, E.J. Cussen, T.J. Prior, M.J. Rosseinsky, Acc. Chem. Res. 38 (2005) 273.
[7] S.L. Stupp, P.V. Braun, Science 277 (1997) 1242.
[8] C.D. Wu, A.G. Hu, L. Zhang, W.B. Lin, J. Am. Chem. Soc. 127 (2005) 8940.
[9] L. Pan, H.M. Liu, X.G. Lei, X.Y. Huang, D.H. Olson, N.J. Turro, J. Li, Angew. Chem. Int. Ed. 42 (2003) 542.
[10] G.J. Halder, C.J. Kepert, B. Moubaraki, K.S. Murray, J.D. Cashion, Science 298 (2002) 1762.
[11] O.M. Yaghi, M. O'Keffe, N.W. Ockwing, H.K. Chae, M. Eddaoudi, J. Kim, Nature 423 (2003) 705.
[12] X. Bu, P. Feng, G.D. Stucky, Science 278 (1997) 2080.
[13] G. Ferey, C.M. Draznieks, C. Serre, F. Millange, J. Dutour, S. Surble, I. Margiolaki, Science 309 (2005) 2040.
[14] (a) J. Zhang, R. Liu, P.Y. Feng, X.H. Bu, Angew. Chem. Int. Ed. 46 (2007) 8388;
(b) Z. Lin, A.M.Z. Slawin, R.E. Morris, J. Am. Chem. Soc. 129 (2007) 4880.
[15] (a) C. Yang, X.P. Wang, M.A. Omary, J. Am. Chem. Soc. 129 (2007) 15454;
(b) I. Boldog, E.B. Rusanov, A.N. Chermega, J. Sieler, K.V. Domasevitch, Angew. Chem. Int. Ed. 40 (2001) 3435;
(c) J. He, Y.G. Yin, T. Wu, D. Li, X.C. Huang, Chem. Commun. (2006) 2845;
(d) J.P. Zhang, S. Kitagawa, J. Am. Chem. Soc. 130 (2008) 907.
[16] I. Boldog, E.B. Rusanov, A.N. Chernega, J. Sieler, K.V. Domasevitch, J. Chem. Soc. Dalton Trans. (2001) 893.
[17] V.V. Ponomarova, V.V. Komarchuk, I. Boldog, A.N. Chermega, J. Sieler, K.V. Domasevitch, Chem. Commun. (2002) 436.
[18] (a) W.L. Mosby, J. Chem. Soc. (1957) 3997;
(b) I. Boldog, E.B. Rusanov, A.N. Chernega, J. Sieler, K.V. Domasevitch, Polyhedron 20 (2001) 887;
(c) I. Boldog, E.B. Rusanov, J. Sieler, S. Blaurock, K.V. Domasevitch, Chem. Commun. (2003) 740;
(d) J.P. Zhang, S. Horike, S. Kitagawa, Angew. Chem. Int. Ed. 46 (2007) 889.
[19] (a) W.W. Wendlandt, H.G. Hecht, Reflectance Spectroscopy, Interscience Publishers, New York, 1966;
(b) G. Kortüm, Reflectance Spectroscopy, Springer, New York, 1969.
[20] (a) Rigaku (2002), CrystalClear Version 1.35, Rigaku Corporation; Siemens (1994), SAINT Software Reference Manual, Siemens Energy & Automation Inc., Madison, WI, USA;
(b) Siemens, SHELXTLTM Version 5 Reference Manual, Siemens Energy & Automation Inc., Madison, WI, USA, 1994.
[21] A. Bondi, J. Phys. Chem. 68 (1964) 441.
[22] (a) E.B. Rusanov, V.V. Ponomarova, V.V. Komarchuk, H. Stoeckli-Evans, E. Fernandez-Ibanez, F. Stoeckli, J. Sieler, K.V. Domasevitch, Angew. Chem. Int. Ed. 42 (2003) 2499;
(b) K.V. Domasevitch, I. Boldog, E.B. Rusanov, J. Hunger, S. Blaurock, M. Schroder, J. Sieler, Z. Anorg. Allg. Chem. 631 (2005) 1095;
(c) P.V. Ganesan, C.J. Kepert, Chem. Commun. (2004) 2168.
[23] (a) L. Chen, J.B. Lin, J.Z. Gong, A.P. Sun, B.H. Ye, X.M. Chen, Cryst. Growth Des. 6 (2006) 2739;
(b) S. Yamada, M. Yasui, T. Nogami, T. Ishida, Dalton Trans. (2006) 1622;
(c) S.U. Son, K.H. Park, B.Y. Kim, Y.K. Chung, Cryst. Growth Des. 3 (2003) 507;
(d) M. Albrecht, Chem. Eur. J. 6 (2000) 3485.
[24] A.F. Wells, Three-Dimensional Nets and Polyhedra, Wiley-Interscience, New York, 1977.
[25] See the website: ⟨http://rcsr.anu.edu.au/⟩.
[26] (a) V.A. Blatov, L. Carlucci, G. Cianib, D.M. Proserpio, CrystEngComm 6 (2004) 377;
(b) J.P. Zhang, Y.Y. Lin, W.X. Zhang, X.M. Chen, J. Am. Chem. Soc. 127 (2005) 14162;
(c) A. Schier, J.M. Wallis, G. Müller, H. Schmidbaur, Angew. Chem. Int. Ed. 25 (1986) 757.
[27] L. Hou, Y.Y. Lin, X.M. Chen, Inorg. Chem. 47 (2008) 1346.